Journal of Biomedical Optics

BiomedicalOptics.SPIEDigitalLibrary.org

Laser trap ionization for identification of human erythrocytes with variable hemoglobin quantitation

Michele Kelley
James Cooper
Daniel Devito
Robert Mushi
Maria del Pilar Aguinaga
Daniel B. Erenso

SPIE.

Michele Kelley, James Cooper, Daniel Devito, Robert Mushi, Maria del Pilar Aguinaga, Daniel B. Erenso, "Laser trap ionization for identification of human erythrocytes with variable hemoglobin quantitation," *J. Biomed. Opt.* **23**(5), 055005 (2018), doi: 10.1117/1.JBO.23.5.055005.

Laser trap ionization for identification of human erythrocytes with variable hemoglobin quantitation

Michele Kelley,[a,*] James Cooper,[a] Daniel Devito,[a] Robert Mushi,[b] Maria del Pilar Aguinaga,[b,c] and Daniel B. Erenso[a]
[a]Middle Tennessee State University, Department of Physics and Astronomy, Murfreesboro, Tennessee, United States
[b]Meharry Medical College, Meharry Sickle Cell Center, Department of Internal Medicine, Nashville, Tennessee, United States
[c]Meharry Medical College, Department of Obstetrics and Gynecology, Nashville, Tennessee, United States

Abstract. An approach to an established technique that is potentially applicable for a more comprehensive understanding of the electrical properties of red blood cells (RBCs) is presented. Using a high-intensity gradient laser trap, RBCs can be singly trapped and consequentially ionized. The subsequent dynamics of the ionized cell allows one to calculate the charge developed and the ionization energy (IE) through a Newtonian-based analysis. RBCs with two different hemoglobin (Hb) types were ionized. The first sample was identified as carrying Hb HbAA (normal Hb) and the second one was identified as carrying HbAC (HbC trait). By analyzing the charge developed on each cell and several other related factors, we were able to discern a difference between the main Hb types contained within the individual RBC, independent of cell size. A relationship between the charge developed and the IE of the cell was also established based on the electrical properties of RBCs. Thus, we present this laser trapping technique as a study of the electrical properties of RBCs and as possible biomedical tool to be used for the differentiation of Hb types. [DOI: 10.1117/1.JBO.23.5.055005]

Keywords: red blood cells; laser trapping; cell mechanics; dielectrophoresis.

Paper 180110RR received Feb. 19, 2018; accepted for publication May 16, 2018; published online May 30, 2018.

1 Introduction

The mechanical properties of human red blood cells (RBCs) have been the subject of extensive studies[1–23] as these properties are determinative of the biological function of these cells. Many of these studies are based on a variety of experimental strategies to probe the mechanics of single RBCs. These strategies include laser trapping (LT),[1–9] micropipette aspiration,[10] atomic force microscopy,[11] ektacytometry,[12] diffraction phase microscopy,[13] and magnetic twisting cytometry.[14] A few recent studies have also reported on the characterization of membrane damage and fatigue in RBCs under cyclic loading using shear flow in a narrow microfluidic channel.[15–23]

The mechanical properties of the RBCs depend on the type of the negatively charged hemoglobin (Hb) molecules that make up the majority of the cytoplasm of the RBCs.[5,6] High-performance liquid chromatography (HPLC)[24] is commonly used to identify and quantitate the different Hb types present in RBCs in a given blood sample. HPLC techniques employ principles of ion-exchange chromatography and spectrophotometry. In this technique, a few microliters of whole blood are hemolyzed to break the membrane of the RBCs and release the Hb molecules from the cytoplasm. Then, the blood is injected into a positively charged column. At a moderately alkaline pH, a cationic exchange occurs between the column and the Hb molecules. In cationic exchange HPLC, the most common Hb molecules elute in the following order: HbF, HbA, HbS, and HbC. HbF has the weakest and HbC has the strongest negative charge. When the hemolysate is injected into the positively charged HPLC column, the HbF type will bind weakly and be eluted quickly from the column whereas the HbC type will bind strongly and be retained longer on the column. This HPLC technique has been widely used for Hb identification and quantitation of Hb variants for hemoglobinopathy screening, as well as for the monitoring of HbS levels in patients with sickle cell disorders (SCD).

An alternative technique that can potentially be utilized for similar applications is the LT technique.[25] LT is an optical technique capable of conveniently trapping and manipulating living[1–9] or nonliving[26] dielectric particles whose dimensions range from tens of nanometers to tens of microns. A few studies have focused on the biomedical applications of the LT technique related to SCD.[4–7] These studies primarily demonstrated the use of the LT to measure the elasticity of the RBCs for studying the efficacies of the various types of therapy used to treat SCD. To highlight a few, the efficacy of hydroxyurea therapy (an FDA-approved drug to treat SCD) has been studied by measuring the properties associated with the elasticity of the RBCs using the LT technique.[5] Recently, we have also reported a similar application for measuring efficacies in blood transfusion therapy for SCD.[6]

Our studies in human RBCs have been primarily based on the relative biophysical deformations resulting from direct trapping of individual cells as the power of the trap increases without compromising the integrity of the cells. During these studies, we observed that the cells respond very differently when they are trapped with a high-power (>50 mW) trap as opposed to

*Address all correspondence to: Michele Kelley, E-mail: mk3g@mtmail.mtsu.edu

a lower power. This led us to the discovery that an RBC trapped at high power undergoes hemolysis, becomes charged, and is consequently ejected from the trap. The time that each cell takes to be ionized (charged), the corresponding ionization energy (IE), and charge developed on the cell depend on the Hb type that the cell is composed of, as different Hb types carry a different magnitude of charge. Recently, using BT20 breast cancer cells we have demonstrated that the IE and the charge developed can be determined at single cell level.[27]

In this study, we present yet another application of single-cell ionization for comparing and contrasting RBCs with different Hb types. Using RBCs from a normal Hb blood sample (HbAA) and an HbC trait blood sample (HbAC), we have demonstrated the ionization of RBCs using the LT technique. The properties associated with the time for ionization, the IE, and the estimated charge resulting from ionization were measured.

2 Materials and Methods

A detailed description of the experimental design and setup for the LT can be referred to our previously reported studies on a similar biomedical application of the LT in RBCs.[6,27] The basic elements of the experimental setup and the procedures relevant to this study are briefly described. These include the laser, the microscope equipped with a high numerical aperture objective lens (OL), a computer-controlled digital camera (DC), and piezo-driven mechanical stage. The laser is a linearly polarized infrared diode laser that generates 5 W at 1064 nm. The power is controlled by a combination of a $\lambda/2$-wave plate and a polarizer. After the laser beam is expanded, collimated, and aligned, it is coupled to an inverted microscope (Olympus IX 71) through its laser port and redirected for a normal incidence angle at the center of the back of the OL using a dichroic mirror positioned at 45 deg inside the microscope. The OL is used to focus the laser beam on the focal plane of the microscope stage. The microscope stage is equipped with computer-controlled piezo-driven stage (PS) for housing and controlled movement of the slide, as well as a DC for live two-dimensional bright-field contrast imaging.

Blood samples carrying HbAA and HbAC Hb types were obtained from the Meharry Sickle Cell Center (MSCC) at Meharry Medical College (MMC), Nashville, Tennessee. A biological material transfer agreement was processed between both institutions involved, Middle Tennessee State University (MTSU) and MMC. For each of these blood samples, the relative percentage quantitation of the different Hb types was performed at the MSCC using HPLC. The normal blood sample contained HbA (97.7%) and HbA2 (2.3%), and the blood sample from the HbAC individual contained HbA (55.05%), HbC (40.35%), HbA2 (3.2%), and HbF (1.4%). Each of the blood samples was diluted 1:1000 with fetal bovine serum for processing at MTSU.

The diluted blood samples were placed on a well-slide and mounted on the PS of the microscope. Using the DC, we took an image of the cell when free and lying on the bottom of the slide. We then opened the gate at the laser port of the microscope and trapped the cell. Successive images of the cell were taken by the DC at a fixed frame-grabbing rate for 2 min beginning the instant the cell was trapped. After some time at sufficiently high power, the cell membrane ruptured, and the cell became charged. Such time-dependent charge interacts with the electromagnetic fields of the laser forming the trap that results in a strong electromagnetic force that exceeds the intensity gradient

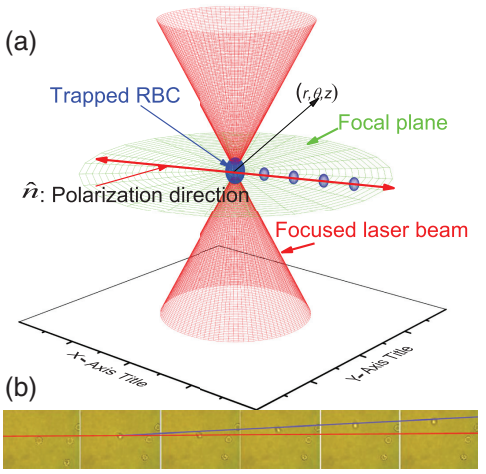

Fig. 1 (a) Schematic representation of a trapped RBC and (b) successive images describing a charged RBC ejected from the trap.

trapping force. At this stage, the cell was ejected from the trap along the linear polarization direction of the laser. A schematic and real live successive images illustrating this process are shown in Fig. 1.

This procedure was carried out for five cells per slide for both blood samples. We considered two power strengths, 128 and 153 mW, at the trap location.

The diameter of each cell before it was trapped and the displacement from the center of the trap after it was ejected (Fig. 1) as a function of time were measured in pixels from the images captured during the process using image analysis programming software, ImageProplus. The time was determined from the frame-grabbing rate of the DC. The measurements in pixels were converted into meters using a conversion factor of 7.27×10^{-8} m/pixel. The conversion factor[27] was determined by measuring the images of silicon beads that had a known diameter (3.1×10^{-6} m) using Image-Pro Plus 6.2.

3 Results and Discussion

3.1 *Ionization*

3.1.1 *Ionization mechanism*

The cytoplasm of an RBC predominantly contains the negatively charged Hb biomolecule. The cell membrane is composed of proteins and a phospholipid bilayer. The phospholipid bilayer membrane is an insulator made of bound charges. Under a strong applied electric field, these bound charges can become extremely polarized. The force of an external electric field, E_o, causes the dipoles in the material to align with the electric field. The alignment of the dipoles decreases the external electric field to $E = E_o/\varepsilon_r$, where ε_r is the dielectric constant of the cell membrane. When the cell is exposed to an oscillating electric field of low frequency, the dipoles will oscillate in resonance with the electric field. However, under the influence of an extremely high electric field oscillating at extremely high frequency, such as the laser forming the trap, the bound charges can no longer be in resonance. The dipoles fail to respond in time to realign before the field reverses direction. Physically, in this strong external electric field, the cell's conductance and permeability increase rapidly.[28] At a certain strength of electric field, the cell will undergo irreversible dielectric breakdown

of the membrane. This process mechanically ruptures the cell.[29,30] Therefore, negatively charged Hb molecules in the cytoplasm, accelerated by the incident electric field of the laser trap, would gradually be driven out of the cytoplasm leaving an oppositely and continually charging cytoskeleton—"the ghost cell." Consequently, the electrostatic force on "the ghost cell" due to the electric field of the laser forming the trap is growing stronger and stronger. The charged particles are driven out of the cytoplasm after the membrane breaks down. At some point, the electrostatic force would be greater than the intensity gradient force of the laser trap as the cell is highly ionized. Consequently, the cell will be ejected from the laser trap.

3.1.2 *Ionization period*

The period of time that each cell took to get ionized and ejected from the trap at fixed power is not the same even for the blood with the same type of Hg. The higher the power, the shorter the time the cell took to be ionized and ejected from the trap. We analyzed the distribution of the period of time for ionization for both blood samples with HbAA and HbAC types. From the images captured, we determined the period from the instant the cell entered to the time it was ejected from the trap using the image capturing rate of the DC. The results are shown in Fig. 2(a) at 128 mW and Fig. 2(b) at 153 mW measured at the trap location. For the RBCs from the blood of the HbAA type, the average periods are $\sim 22 \pm 7$ s and $\sim 16 \pm 5$ s whereas, for those RBCs from the blood with HbAC type are $\sim 19 \pm 5$ s and $\sim 12 \pm 6$ s at 128 and 153 mW, respectively.

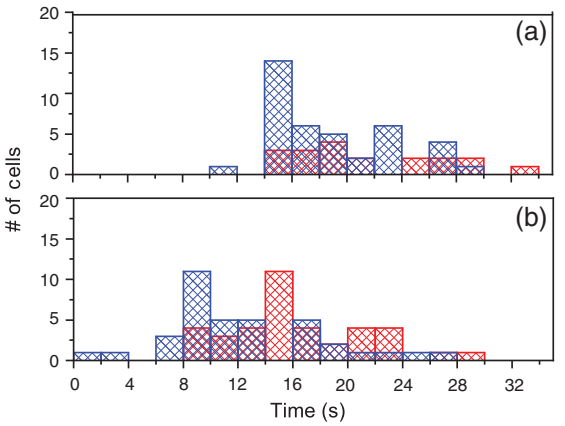

Fig. 2 The ionization period distribution at (a) 128- and (b) 153-mW power at the trap location. Red is for a blood with HbAA type and blue is with HbAC type.

3.1.3 *Ionization energy*

The IE, the radiation dose (RD), and the relation of IE and RD to the sizes of the cells measured by the diameter of the cells were studied. The IE was determined from the measured incident power at the trap location (P) and the corresponding ionization period for each cell (T) is shown in Fig. 2, using $\mathrm{IE} = P \times T$. P_T is measured by covering the tip of the OL about half a centimeter away with a laser power meter head (Coherent® FieldMax II-TOP Laser Power). The period T is determined from two images captured when the cell just got into and ejected out of the trap. The recorded time for these images and the camera image capturing rate were used to calculate T. Commonly, RD is measured by the amount of energy absorbed per unit mass. Here, RD was studied using not the amount of the absorbed energy by each cell but rather using the incident energy. It was necessary to use the area instead of the mass (m) as the power measured here is the incident power, not the absorbed power. Such a measurement of the absorbed power requires covering the slide with a laser power meter, which was technically difficult as it totally blocks the imaging light needed for capturing the images. The RD was then calculated using: $\mathrm{RD} = \mathrm{IE}/A$ in units of $\mathrm{mJ}/\mu\mathrm{m}^2$.

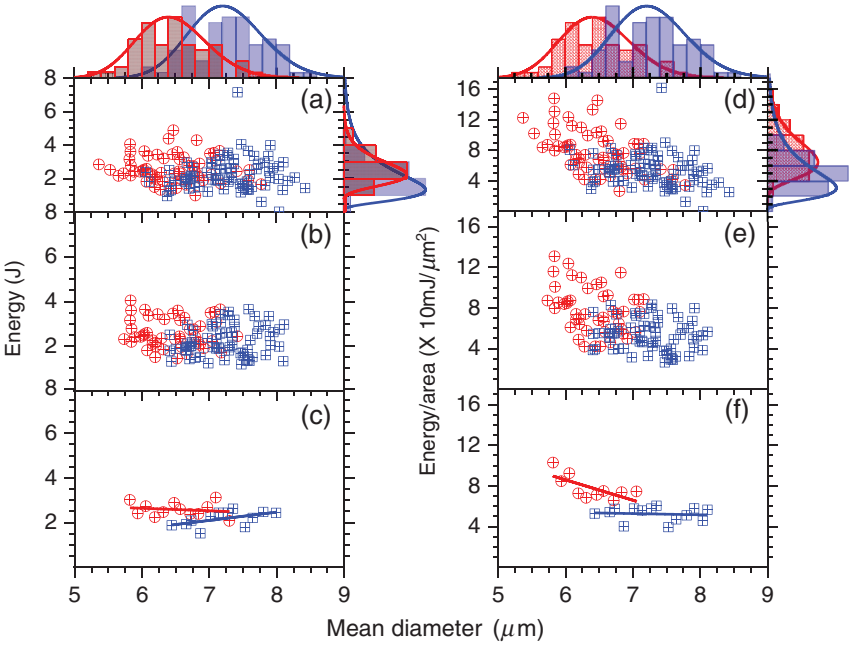

Fig. 3 The (a)–(c) IE and the (d)–(f) RD versus diameter for HbAA (red) and for HbAC (blue). (a) and (d) are for all cells; (b) and (e) are the reduced data; and (c) and (f) are the grouped averages with the best-fitting lines.

The relations of the IE and RD to the size of the cell were studied using the average diameter measured prior to trapping.

The result for the IE versus the diameter for each RBCs from the two blood samples at the two powers (128 and 153 mW) for the HbAA (red) and for HbAC (blue) are shown in Fig. 3(a). Using the same color coding, we also show the distribution for the diameter and the IE for both blood samples in Fig. 3(a) using histograms. The basic statistical parameters are also shown in Table 1. A total of 59 from the HbAA and 77 from HbAC blood samples were analyzed. For these blood samples, the average IEs are 2.6 ± 0.8 J and 2.2 ± 0.9 J and the average diameters are 6.5 ± 0.5 μm and 7.3 ± 0.5 μm, respectively. To compare the result for the two blood types with different Hb make up, we made an analysis that is based on a statistically valid data reduction using graphical data analysis programing software, OriginPro 2018. The results for the reduced data are shown in Fig. 3(b) using the same color coding for the two blood samples for both powers. These data were obtained by sorting in ascending order first by the IE and removing the three maximum and minimum values. These data were sorted again in ascending order, but this time by diameter. Again, the three minimum and maximum values were eliminated from the list that leads to a total of 47 cells for HbAA and 65 for HbAC as shown in Fig. 3(b). These results for each blood samples were grouped with an increment of 0.13 μm. For each group, the average diameter and the corresponding average IE were calculated. The results are shown in Fig 3(c) using the same color coding. The best-fitting linear curve shown in Fig. 3(c) clearly shows the IE for HbAA is greater than HbAC, independent of the size of the cells.

A similar procedure was used to study the relationship between the RD versus the diameter of the cells. The results for the HbAA and HbAC using the same color coding are shown in Figs. 3(d) and 3(f). Figure 3(d) shows the RD versus the diameter for all cells and the corresponding distributions shown by the histograms for the RD and the diameter for both HbAA and HbAC. The average RD for HbAA and HbAC is 79.4 ± 2.8 mJ/μm^2 and 53.1 ± 2.2 mJ/μm^2, respectively. The reduced data obtained following the same procedure used for the IE are shown in Figs. 3(e) and 3(f). This shows that the RD for RBCs from the HbAA blood sample is higher than from the HbAC blood sample. As we can see from the Hb quantitation by HPLC given in Table 1, the HbAA blood sample contained predominantly HbA (97.7%), which is the normal Hb. On the other hand, HbAC blood sample contained HbA (55.05%) and HbC (40.35%). HbC is a structural variant of normal Hb A

Table 1 Blood sample Hb quantitation by HPLC and basic statistical parameters for the physical quantities studied.

Relative % of each Hb for HbAA blood sample		Relative % of each Hb for HbAC blood sample	
HbA (%)	97.7	HbA (%)	55.05
HbA^2 (%)	2.3	HbA2 (%)	3.2
HbC (%)	0	HbC (%)	40.35
HbS (%)	0	HbS (%)	0
HbF (%)	0	HbF (%)	1.4

Basic statistical physical parameters

Quantities	No. of cells	Mean	STD	Sum	Min	Median	Max
			HbAA blood sample				
Diameter (μm)	59	6.46	0.52	381.25	5.36	6.46	7.77
IE (J)	59	2.6	0.81	153.55	0.98	2.42	4.88
RD ($10 \times$ mJ/μm^2)	59	7.94	2.83	468.55	2.66	7.62	14.79
Z number(×10)	59	7.81	4.82	460.79	1.55	6.99	27.2
Z number per area (Z/μm^2)	59	2.36	1.46	139.58	0.45	1.9	6.82
			HbAC blood sample				
Diameter (μm)	77	7.27	0.54	559.55	6.06	7.29	8.43
IE (J)	77	2.23	0.95	171.48	0.02	2.01	7.14
RD ($10 \times$ mJ/μm^2)	77	5.31	2.19	408.93	0.05	5.3	16.18
Z number (×10)	72	21.6	7.4	1555.69	9.72	20.84	45.42
Z number per area (Z/μm^2)	72	5.17	1.93	372.35	2.02	4.86	11.41

(HbA) caused by an amino acid substitution of lysine for glutamic acid at position six of the beta Hb chain. HbC is less soluble than HbA in RBCs. Crystal formation may result, leading to increased cellular rigidity.[31] This could lead to increased (i.e., lesser energy to break the membrane) fragility for RBCs from the HbAC blood sample than those from HbAA. Thus, the smaller RD for HbAC than HbAA agrees with the expected properties of RBCs with HbC. Figure 3(e) also shows a decrease of RD/area for HbAA as the diameter increases. However, for those RBCs with HbAC, the decrease is insignificant and hardly such a correlation can be made. Further study beyond the scope of this paper would be required to ascertain a relationship between the two.

3.2 *Postionization*

3.2.1 *All cell dynamics*

We analyzed the images of the cell from the instant it was ejected from the trap until it disappeared from the view range of the DC. From these images, we measured the displacement of each cell from the center of the trap as a function of time. The displacement was measured using Image-Pro Plus 6.2, and the corresponding time was determined from the DC frame-grabbing rate following a similar procedure discussed earlier. The resulting kinematics of the cells postionization is shown in Fig. 4. The displacement as a function of time for the RBCs from HbAC and for RBCs from HbAA is shown in Figs. 4(a) and 4(b), respectively. In these figures, the results for the cells ejected from the higher (153 mW) and lower (128 mW) power trap are represented in black and green, respectively. In terms of the differences of power, the result displays no significant change in either of the two. However, comparison of Figs. 4(a) and 4(b) clearly show a distinct difference between HbAC and HbAA. The speed of each ejected cell as a function of time can be determined from the displacement versus time curves fitting to trajectory for each cell individually. Qualitatively, we see from the slopes of the displacement versus time graphs in Figs. 4(a) and 4(b), the speed of the RBCs from HbAC is higher than those from HbAA blood. Based on this qualitative observation, we can argue that the RBCs from HbAC have developed a higher charge relative to the cells from HbAA at the instant it got ejected from the trap. We have discussed the mechanism of the ionization and how, in general, the charges developed in the RBCs by a fast oscillating electric field of a high-power laser forming the trap. Next, we will make a qualitative and quantitative explanation of why the charge magnitude is expected to be higher for the RBCs from HbAC than HbAA blood.

As the cell membrane breaks down, the ions in the cytoplasm would be free and can be driven out by the electrical force due to the electric field of the laser. These ions are predominantly the negatively charged Hb molecules for the RBCs. As the Hb molecules are driven out of the cytoplasm, the cell gradually becomes positively charged. The magnitude of this charge depends on the amount of negatively charged Hb molecules driven out. All Hb carry a variable net negative charge with

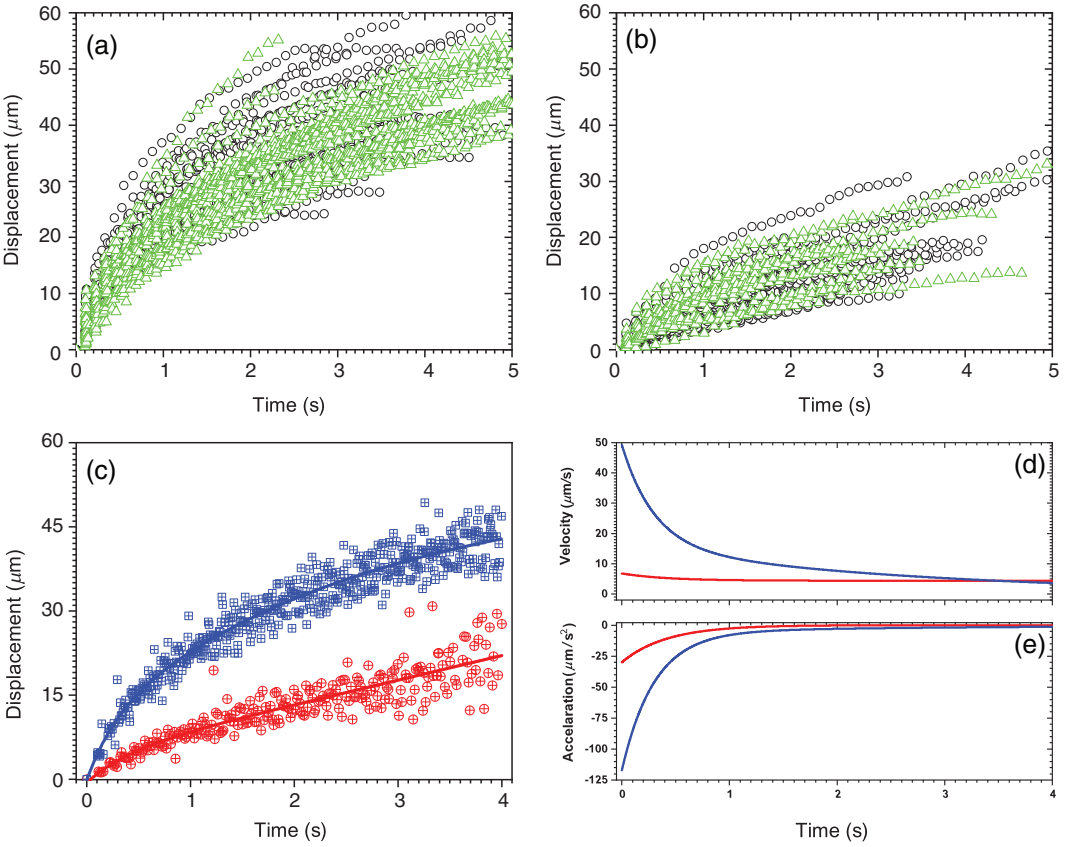

Fig. 4 The displacement of the ejected charged cell as a function of time for (a) HbAC and (b) HbAA blood for all cells at 153 mW (black) and 128 mW (green). The (c) reduced displacement, (d) velocity, and (e) acceleration versus time, HbAC (blue), and HbAA (red).

magnitude distinctive to the specific type of Hb. The common Hb types are HbF, HbA, HbS, and HbC. In this order, HbF has the smallest and HbC has the highest negative charge. Thus, since HbC carries a higher negative charge than HbA, the RBC from HbAC blood seems to develop a higher positive charge than the RBC from HbAA. The Hb quantitation by HPLC showed that the HbAA blood sample contained predominantly HbA (97.7%), whereas the HbAC blood contained HbA (55.05%) and HbC (40.35%). Higher charge means the electrical field of the laser creates stronger electrical force that results in the ejection of the cell at a higher speed. For this reason, the results in Figs. 4(a) and 4(b), qualitatively, showed a higher slope (or speed) for the RBCs from the HbAC than from HbAA blood.

To describe the difference in the magnitude of the charge developed in the RBCs, we have made a further analysis to determine the average kinematic equations describing the dynamics of the ejected cells in each sample. These analyses are based on a statistically and physically acceptable data reduction method using OriginPro 2018. The combined results for the displacement of each cell as function of time at the two powers [Figs. 4(a) and 4(b)] were sorted by the time values. We then eliminated all the displacement versus time values in the time interval >4 s. The remaining results were subgrouped by time increment of 15 ms for each set of data. For each subgroup, the averages for the displacement and the corresponding time were calculated. Equations for the reduced displacement versus time values were determined by nonlinear curve fitting using OriginPro 2018. The results are shown in Fig. 4(c), for RBCs from HbAC labeled blue and HbAA labeled red. The fitting curves shown in Fig. 4(c) were determined using OriginPro 2018 and differentiated with respect to time to determine the average speed and acceleration. The results for the speed are shown in Fig. 4(d) and the acceleration in Fig. 4(e). Immediately after ejection, Fig. 4(d) shows that the cells from the HbAC blood sample are ejected from the trap at about five times the average speed of the RBCs from the HbAA type. This confirms that there is higher charge on the RBCs with HbAC type than those with HbAA blood. This is expected because higher ejection speed is a result of the action of a stronger driving electrical force due to the high charge developed on the cell during the ionization process. The result in Fig. 4(d) also displays as the cells continue to move away from the center of the trap, the speed sharply decreases in both cases, though it becomes sharper for RBCs with HbAC type than the RBCs with HbAA type.

There are two main reasons for the decrease in the speed. One is due to the Gaussian nature of the laser forming the trap. For a Gaussian laser trap, the strength of the electric field sharply decreases from the center. This significantly reduces the contribution of the electrostatic force acting on the ionized cell. The second reason is the viscous drag force, which is proportional to the velocity. We also note that the rate at which the speed decreases, as shown by the acceleration versus time graph in Fig. 4(e), shows the effect of these two forces. This net force acting on the cells, which is proportional to the acceleration, is negative in both cases confirming the average speed is decreasing. This force is the net result of the intensity gradient and drag forces opposing the movement of the ejected cells. Its magnitude is stronger for the RBCs from HbAC than HbAA when we compare the two at the same corresponding time.

3.2.2 *Theoretical model*

To determine the magnitude of the charge on each cell, we have developed a theoretical model. The magnitude of the electric field (E_o) and the magnetic field (B_o) of the laser forming the trap is critical to find this charge. Taking the magnetic permeability of the medium to be that of a free space, μ_o, the Poynting vector of the laser beam, $S = E_o B_o/\mu_o$, with the recorded power at the trap location (P) can be used to determine the magnitude of the electric field. By expressing B_o in terms of E_o and the speed of the laser beam in the cell medium, v ($B_o = E_o/v$), one can easily find that

$$E_o = \sqrt{\frac{2Pv\mu_o}{A}}. \tag{1}$$

The beam size, A, was calculated using the method described in one of our previous papers.[6,27] Using Eq. (1), the average electric field was found to be 21,799.2 N/C for the lower 128-mW power and 23,879.9 N/C for the higher 153-mW power. These electric field strengths are at the location of the trap. It should be noted that Eq. (1) is an expression for the average electric field.

An RBC is a micron-sized negatively charged dielectric living object. The membrane contains proteins and glycoproteins embedded in a fluid lipid bilayer. Sialylated glycoproteins of the RBC membrane are responsible for the negatively charged surface that creates a repulsive electrostatic force between cells preventing interactions between RBCs.[32] Let the total surface charge on the RBC be q_o. When this cell is captured by the laser trap, the fields of the laser oscillating at optical frequency cause the dipoles within the cell and the surface charges to oscillate at the optical frequency. At sufficiently high power, after some period of time, such oscillations rupture the cell membrane resulting in free negatively charged Hb and an oppositely charged cell. Let the free charge developed on the cell as a result of the membrane rupture be q. This charge is created only in the instant that the membrane ruptures, effectually giving rise to the time dependence of the charge density. Considering a spherical model for an RBC with radius r_o, the charge density on the RBC can be approximated using the Dirac delta function

$$\rho(r,t) = \frac{q_o}{4\pi r_o^2}\delta(r - r_o) + q\delta(r)T\delta(t), \tag{2}$$

where T is the period when the cell was in the trap before the membrane ruptured. In Fig. 1, we have shown a schematic for the laser beam trapping the RBC. The laser propagating along the z-direction is a linearly polarized beam. By aligning the x-axis with the polarization direction, the time averaged force on the RBC using the charge density in Eq. (2) can then be expressed as

$$\begin{aligned}\langle \vec{F}_{\mathrm{EM}} \rangle = \mathrm{Re}\Bigg\{ & \frac{q_o}{4\pi}\int_V E(\vec{r})\delta(r - r_o)d^3r\frac{1}{T}\int_0^T \left[\hat{x} + \frac{\vec{v}(t)}{c}\times\hat{y}\right] \\ & \times \exp[i(\vec{k}\cdot\vec{r} - \omega t)]\mathrm{d}t \\ & + q\int_V E(r)\delta(r)d^3r\frac{1}{T}\int_0^T \delta(t)\left[\hat{x} + \frac{\vec{v}(t)}{c}\times\hat{y}\right] \\ & \times \exp[i(\vec{k}\cdot\vec{r} - \omega t)]\mathrm{d}t\Bigg\}, \end{aligned} \tag{3}$$

where the first term represents the interaction of the preexisting surface charge, q_o, and the second term represents

the interaction of the charge resulted from the membrane breakdown, q, with the electric field and magnetic field of the laser beam. In each term, the first integration is over the volume of the charge (RBC), V, and the second integral is over a period, T. The constants are as follows: c describes the speed of light in the medium, $v(t)$ is the velocity of the cell, the vector k is the wave vector (which is directed along the z-axis), ω is the frequency of the laser, the vector r represents the position of the charge at a given time t while the cell is in the trap, and E is the electric field amplitude of the Gaussian laser beam. Noting that the magnitude of the velocity of the charge, $v(t)$, where

$$\vec{v}(t) = \frac{d\vec{r}}{dt} = v_x(t)\hat{x} + v_y(t)\hat{y} + v_z(t)\hat{z} \tag{4}$$

is negligibly small compared to c, the magnetic force contribution in Eq. (3) can be dropped and Eq. (3) can be rewritten as

$$\langle \vec{F}_E \rangle = \mathrm{Re}\left\{ \frac{q_o}{4\pi} \int_V E(\vec{r})\delta(r - r_o) d^3 r \frac{1}{T} \int_0^T \exp[i(\vec{k}\cdot\vec{r} - \omega t)] \mathrm{d}t\hat{x} + q \int_V E(r)\delta(r) d^3 r \frac{1}{T} \int_0^T \delta(t) \exp[i(\vec{k}\cdot\vec{r} - \omega t)] \mathrm{d}t\hat{x} \right\}. \tag{5}$$

In the above equation, the electric force due to the surface charges qo is zero as the integral over time in the first term returns a null value. Therefore, from Eq. (5), using the properties of the Dirac delta function, one can easily find the force

$$\langle \vec{F}_E \rangle = qE_o\hat{n}, \tag{6}$$

where E_o is the amplitude of the electric field and generalized the polarization direction of the laser by n. The result in Eq. (6) shows that the RBCs are ejected along the direction of polarization of the laser beam.

We consider three forces acting on the cell: the electrostatic force, F_E, the drag force, F_D, and trapping force of the laser, F_T. Each cell was considered to be a cylinder with mass m, in a trajectory away from the trap at a distance r from the center of the trap, at a given time t. The cross-sectional area was found as well as the volume for the RBCs.

Both the electrical and the trapping forces depend on the electric field strength at the position of the cell. As previously stated, the laser beam can be correctly approximated to be Gaussian. One can thus express the electric field of laser, as a function of the distance from the trap as

$$E(r) = E_o \exp(ikr) \exp(-r^2/\omega_o^2), \tag{7}$$

where ω_0 is the beam waist of the laser and E_o is the magnitude of the electric field as found by Eq. (1). The trapping force is proportional to the gradient of the electric field in Eq. (2) squared. The drag force due to the viscosity of the medium is equivalent to

$$F_D = -\beta \frac{dr}{dt}, \tag{8}$$

where Stokes' law was used to describe the drag coefficient of a sphere. Just after the cell is ejected from the trap, the equation of motion can be written as

$$m\frac{d^2r(t)}{dt^2} = qE_o - \beta\frac{dr(t)}{dt} + \frac{1}{2}\alpha\nabla\left[E_o e^{ikr} e^{\frac{-r(t)^2}{\omega_o}}\right]^2. \tag{9}$$

In the above equation, the first term describes the magnitude of the electrostatic force created on the cell due to the charge, q, produced on the cell when the membrane ruptures and the electric field of the laser beam forming the trap. The second term is the drag force on the cell, where β is the drag coefficient and $r(t)$ is the displacement of the cell as measured from the center of the trap. The last term is the intensity gradient force of the trap on the cell. The constant ω_0 is the beam waist of the laser and α depends on the relative electrical susceptibility of the cell with respect to the suspension medium and the physical properties, such as the size and shape of the cell after it is ionized.

A physically justifiable approximation was made in order to solve this differential equation analytically. Series expansions were taken of the electrical and trapping forces. Over the range in which the trajectory was measured, the trapping force does not vary significantly; thus, only terms in first order r were retained, where k represents the trapping coefficient. Thus, our model is like a charged damped harmonic oscillator in a uniform electric field with spring constant k. The approximate equation of motion becomes

$$m\frac{d^2r(t)}{dt^2} = qE_o - \beta\frac{dr(t)}{dt} - kr(t), \tag{10}$$

and the solution of which was found to be

$$r(t) = \frac{E_o q}{k}\left\{1 - e^{-\beta t/2m}\left[\cosh\left(\frac{\sqrt{\beta^2 - 4\ \mathrm{km}}}{2m}t\right) + \frac{\beta}{\sqrt{\beta^2 - 4\ \mathrm{km}}}\sinh\left(\frac{\sqrt{\beta^2 - 4\ \mathrm{km}}}{2m}t\right)\right]\right\}. \tag{11}$$

By measuring several cells diameter's before and after the ionization process, we found an average reduction factor of 0.43. This was used to calculate a reduced mass and drag coefficient. The average reduced masses of the HbAC and the HbAA cells, modeled as spheres, were found to be 1.49×10^{-14} kg and 1.26×10^{-14} kg, respectively. The drag coefficient β was $\sim 2.77 \times 10^{-8}$ Ns/m and 2.62×10^{-8} Ns/m for HbAC and HbAA, respectively, where the viscosity of the medium was assumed to be in the same order of water, which at room temperature is 1.002×10^{-3} Ns/m^2. Therefore, the reduced mass, m, drag coefficient, β, and electric field, E_0, were known for each cell; the values of the charge on the cell, q, and the trapping "spring" constant, k, were unknown. The numerical model fitting function NonlinearModelFit in Mathematica was used to fit Eq. (6) to each cell's trajectory [the displacement versus time shown in Figs. 4(a) and 4(b)], therefore finding the values of q and k for each cell. Physically, Eq. (6) must represent an exponential solution, not oscillatory. This requires that maximum values of k, the trapping constant, to be 0.013 for both HbAA and HbAC. This physical restraint was implemented by letting the NonlinearModelFit function start looking for k at a several orders of magnitude below these values. This was done as the function increments the test values for k such that the initial value of k must be set well below the predicted value. For each cell of both the HbAA and HbAC type, the unknown constants of the charge on the cell, q, and the

trapping coefficient, k, were found. The determinant of agreeance, R^2, had a mean value of 0.98 for HbAA and 0.97 for HbAC.

3.2.3 *Charge comparison*

To compare the charges, q, developed for the RBCs in the HbAA and HbAC blood samples, we have studied the charge and the charge per unit area as function of the diameter for each cell. Using the same color coding we used for the IE and RD, the results are shown in Fig. 5. To describe the magnitude of the charge, we used the Z number,[33] which is the magnitude of the charge divided by the magnitude of the charge of an electron. The result for charge (Z) and the charge per unit area (Z/A) for a total of 59 (HbAA) and 76 (HbAC) RBCs were determined. The results as a function of the diameter of each cell are shown in Figs. 5(a) and 5(d), respectively. Figures 5(a) and 5(d) also display the histograms showing the distributions of these values. The values for the basic statistical parameters are listed in Table 1. The Z number values range from 16 to 272 with an average of 78 ± 48, and the Z number per area ranges from 0.5 to $6.82/\mu m^2$ with an average of $2.36 \pm 1.46/\mu m^2$ for the RBCs from the HbAA blood sample. The Z number of the RBCs from the HbAC ranges from 97 to 454 with an average of 216 ± 74, and the Z number per area ranges from 2.0 to $11.4/\mu m^2$ with an average of $5.17 \pm 1.9/\mu m^2$. The average diameter of the RBCs considered here is 6.5 ± 0.5 μm for the HbAA and 7.3 ± 0.6 μm for HbAC blood samples. The same statistical data reduction procedure used for the IE and RD was also used for the Z number and Z/A. The results for the reduced data are shown in Figs. 5(b) and 5(c) for the Z number and in Figs. 5(e) and 5(f) for Z/A. From these reduced data graphs, we note that the magnitude of the charge developed on the RBCs from the HbAC blood sample is higher than those from the HbAA independent of the size of the cells. The corresponding best-fit line for the reduced data in Fig 5(f), with an increase in the size of the cells, predicts a decrease in Z number per area for both RBCs from HbAA and HbAC blood samples.

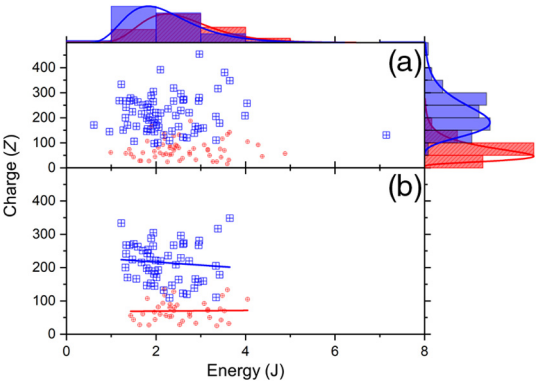

Fig. 6 The charge as a function of the IE for (a) all cells and (b) the reduced data.

It is important to study the relationship between the charge and the IE. The results for the Z number versus the IE are shown in Fig. 6. The results in Fig. 6(a) show Z versus IE for all the RBCs, for a total of 59 from the HbAA (red) and 76 from HbAC (blue), considered for this analysis. It also contains the histograms representing the distributions for the IE (on the horizontal axis) and the charge (on the vertical axis). The reduced data shown in Fig. 6(b) were obtained using a similar approach discussed earlier that included the size, IE, and Z values. These values for the RBCs in each blood sample were first sorted in ascending order by Z values and the three maximum and three minimum values were eliminated. The remaining data were further sorted in ascending order by IE and then diameter followed by elimination of three maximum and three minimum

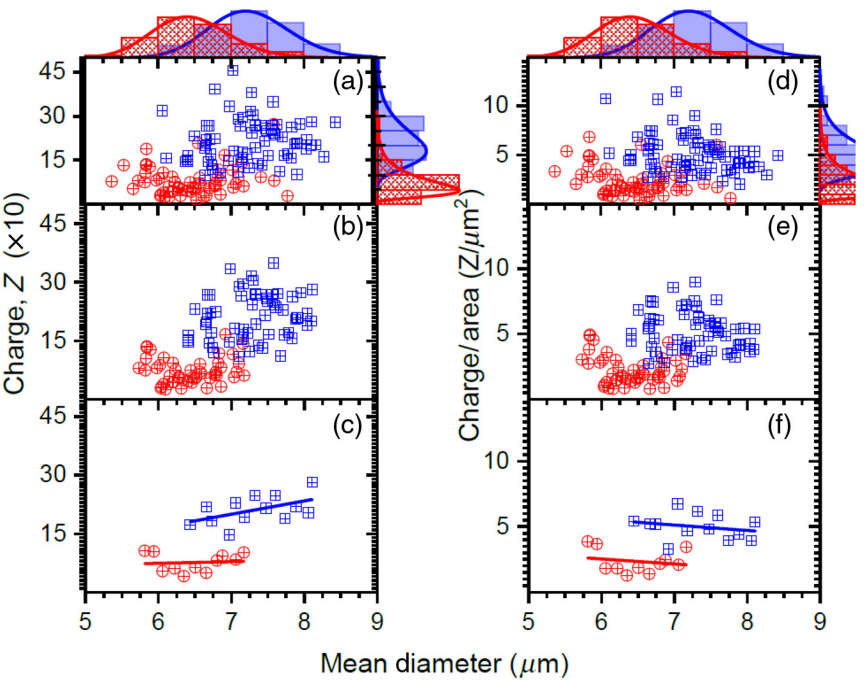

Fig. 5 (a)–(c) The charge measured by Z number and (d)–(f) the charge per area (Z/A) versus diameter for HbAA (red) and for HbAC (blue). (a) and (d) are for all cells; (b) and (e) are the reduced data; and (c) and (f) are the grouped averages with the best-fitting lines.

values in each operation. This has reduced the data to a total of 39 RBCs for HbAA (red) and 54 RBCs for HbAC (blue) blood samples. This is shown in Fig. 6(b) and it shows the result is consistent to what was observed for charge versus diameter, here also the charge versus IE is higher for RBCs from HbAC than RBCs from HbAA. The interesting behavior that we observe here is that the reduced data seem to predict the same charge independent of IE per cell in both cases.

4 Concluding Remarks

Since its invention, more than four decades ago, the LT technique has been extensively used to study the mechanical properties of RBCs. However, it has never been used to uncover the electrical properties of these cells that, in fact, determine the mechanical properties of the cells. In this study, we have shown that the LT technique can be used to study the electrical properties of RBCs and has potential to be applicable for quantitative comparing and contrasting of RBCs with different Hb quantitation. We have demonstrated this application using RBCs from a normal (HbAA) and HbC trait (HbAC) blood samples, which is founded on our previous methodology used for single-cell ionization of BT20 breast cancer cells.[27] RBCs from these two blood samples, for which the Hb quantitation was predetermined using HPLC, were singly trapped and ionized by a high-intensity infrared laser at 1064-nm wavelength. The IE measured by the incident energy on the trapped individual cells and the RD measured by the IE per unit area were determined. Furthermore, the magnitude of the charge developed measured by the Z number and Z number per area was calculated and studied by analyzing the postionization dynamics of the individual cells. The results presented consistently have shown that the RBCs from the blood sample with HbC have higher IE, RD, charge, and charge per area than those RBCs from a normal blood sample. The study has also presented the relation of these quantities to the size of the cells quantified by the average diameter of the individual cells. The results seem to predict there is negligible variation for the average IE and Z and slight decrease for RD and Z per area as the size of the cells increase in both cases. However, we would like to emphasize that it may require further studies to make a conclusive remark for these predictions. On the other hand, the analysis on the relation between the magnitude of the charge developed and IE predict the charge does not seem to change with IE variation in both cases.

Disclosures

The authors have no relevant financial interests in this work and no other potential conflicts of interest to disclose.

Acknowledgments

Partial funding for this activity came from MTSU's URECA, NSF FirstStep Grant and the Department of Health and Human Services/Office of Minority Health (No. MPCMP081013 B OMH-MMC-1-09). The views expressed in written materials or publications and by speakers and spokespersons do not necessarily reflect the official policies of the Office on Minority Health and Health Disparities nor does mention by trade names, commercial practices, or organizations imply endorsement by the U.S. government.

References

1. A. Ashkin, J. M. Dziedzic, and T. Yamane, "Optical trapping and manipulation of single cells using infrared laser beams," *Nature* **330**, 769–771 (1987).
2. F. Bordeleau et al., "Measuring integrated cellular mechanical stress response at focal adhesions by optical tweezers," *J. Biomed. Opt.* **16**(9), 095005 (2011).
3. S. Rancourt-Grenier et al., "Dynamic deformation of red blood cell in dual-trap optical tweezers," *Opt. Express* **18**, 10462–10472 (2010).
4. M. M. Brandão et al., "Elastic properties of stored red blood cells from sickle trait donor units," *Vox Sang.* **85**(3), 213–215 (2003).
5. M. M. Brandão et al., "Optical tweezers for measuring red blood cell elasticity: application to the study of drug response in sickle cell disease," *Eur. J. Haematol.* **70**(4), 207–211 (2003).
6. A. Pellizzaro et al., "Direct laser trapping for measuring the behavior of transfused erythrocytes in a sickle cell anemia patient," *Biomed. Opt. Express* **3**(9), 2190–2199 (2012).
7. R. Solomon et al., "Physical and mechanical properties of the human red blood cells with different hemoglobin types," in *Proc. of the National Conf. on Undergraduate Research (NCUR)*, University of Wisconsin, La Crosse (2013).
8. T. Barnes et al., "Assessment of the elasticity of erythrocytes in different physiological fluids by laser traps," *Opt. Photonics J.* **3**(2), 211–216 (2013).
9. M. Dao, C. T. Lim, and S. Suresh, "Mechanics of the human red blood cell deformed by optical tweezers," *J. Mech. Phys. Solids* **51**(11), 2259–2280 (2003).
10. G. M. Artmann et al., "Micropipette aspiration of human erythrocytes induces echinocytes via membrane phospholipid translocation," *Biophys. J.* **72**(3), 1434–1441 (1997).
11. C. Lim et al., "Experimental techniques for single cell and single molecule biomechanics," *Mater. Sci. Eng. C* **26**(8), 1278–1288 (2006).
12. R. Johnson, "Ektacytometry of red blood-cells," *Methods Enzymol.* **173**, 35–54 (1989).
13. R. Wang et al., "Effective 3D viscoelasticity of red blood cells measured by diffraction phase microscopy," *Biomed. Opt. Express* **2**(3), 485–490 (2011).
14. M. Puig-De-Morales-Marinkovic et al., "Viscoelasticity of the human red blood cell," *Am. J. Physiol. Cell Physiol.* **293**(2), C597–C605 (2007).
15. S. Sakuma et al., "Red blood cell fatigue evaluation based on the close-encountering point between extensibility and recoverability," *Lab Chip* **14**(6) 1135–1141 (2014).
16. S. Hashimoto, "Detect of sublethal damage with cyclic deformation of erythrocyte in shear flow," in *WMSCI 2014, 18th World Multi-Conf. on Systemics, Cybernetics and Informatics, Proc.*, Vol. **2**, pp. 108–113 (2014).
17. H. Engelhardt and E. Sackmann, "On the measurement of shear elastic moduli and viscosities of erythrocyte plasma membranes by transient deformation in high frequency electric fields," *Biophys. J.* **54**(3), 495–508 (1988).
18. H. Engelhardt, H. Gaub, and E. Sackmann, "Viscoelastic properties of erythrocyte membranes in high frequency electric fields," *Nature* **307**(5949), 378–380 (1984).
19. E. Du, M. Dao, and S. Suresh, "Quantitative biomechanics of healthy and diseased human red blood cells using dielectrophoresis in a microfluidic system," *Extreme Mech. Lett.* **1**, 35–41 (2014).
20. I. Guido, M. Jaeger, and C. Duschl, "Dielectrophoretic stretching of cells allows for characterization of their mechanical properties," *Eur. Biophys. J.* **40**(3), 281–288 (2011).
21. J. Chen et al., "Electrodeformation for single cell mechanical characterization," *J. Micromech. Microeng.* **21**(5), 242–540 (2011).
22. L. MacQueen, M. Buschmann, and M. Wertheimer, "Mechanical properties of mammalian cells in suspension measured by electro-deformation," *J. Micromech. Microeng.* **20**(6), 065007 (2010).
23. Y. Qiang, J. Liu, and E. Du, "Dynamic fatigue measurement of human erythrocytes using dielectrophoresis," *Acta Biomater.* **57**, 352–362 (2017).
24. A. Kutlar et al., "Quantitation of hemoglobin components by high-performance cation-exchange liquid chromatography: its use in diagnosis and in the assessment of cellular distribution of hemoglobin variants," *Am. J. Hematol.* **17**, 39–53 (1984).

25. A. Ashkin, "Applications of laser radiation pressure," *Science* **210**(4474), 1081–1088 (1971).
26. D. Erenso et al., "Formation of synthetic structures with micron size silica beads using optical tweezer," *J. Mod. Opt.* **54**(10), 1529–1536 (2007).
27. M. Kelley, Y. Gao, and D. Erenso, "Single cell ionization by a laser trap: a preliminary study in measuring radiation dose and charge in BT20 breast carcinoma cells," *Biomed. Opt. Express* **7**(9), 3438–3448. (2016).
28. J. Weaver and K. Schoenbach, "Biodielectrics," *IEEE Trans. Dielectr. Electr. Insul.* **10**(5), 715–716 (2003).
29. L. Chernomordik et al., "The electrical breakdown of cell and lipid membranes: the similarity of phenomenologies," *Biochim. Biophys. Acta* **902**, 360–373 (1987).
30. U. Zimmermann, G. Pilwat, and F. Riemann, "Dielectric breakdown of cell membrane," *Biophys. J.* **14**, 881–899 (1974).
31. S. Charache et al., "Pathogenesis of hemolytic anemia in homozygous hemoglobin C disease," *J. Clin. Invest.* **46**(11), 1795–1811, (1967).
32. H. P. Fernandes, C. L. Cesar, and M. de L. Barjas-Castro, "Electrical properties of the red blood cell membrane and immunohematological investigation," *Rev. Bras. Hematol. Hemoter.* **33**(4), 297–301 (2011).
33. C. Gary-Bobo and A. Solomon, "Hemoglobin charge dependence on hemoglobin concentration in vitro," *J. Gen. Physiol.* **57**(3), 283–289 (1971).

Michele Kelley is a graduate student at the University of North Carolina at Chapel Hill where she is pursuing her doctorate in physics. She received her BS degree in physics from Middle Tennessee State University in 2016. Her research interests include biomedical optics, medical physics, and imaging.

Maria del Pilar Aguinaga is a tenured professor in the Department of Obstetrics and Gynecology and is the codirector and laboratory director of the Meharry Sickle Cell Center. She received her PhD in biophysics and molecular biology from Kanazawa University Medical School, Kanazawa, Japan, in 1984. Her research interest is in the hemoglobinopathies and women's health. Her clinical interest lies in the diagnosis of hemoglobin disorders, for which she is consulted nationally and internationally.

Daniel B. Erenso is a professor at Middle Tennessee State University. He received his BS and MS degrees in physics from Addis Ababa University in 1990 and 1997, respectively, and his PhD in quantum optics from the University of Arkansas in 2003. He is the author of more than 30 publications. His current research interests include biomedical optics, quantum optics, and quantum information. He is a member of OSA and APS.

Biographies for the other authors are not available.